OPEN ACCESS

University of BRISTOL

Khawaja, BAM., & Cryan, MJ. (2010). Wireless hybrid mode locked lasers for next generation radio-over-fiber systems. *Journal of Lightwave Technology*, *28*(16), 2268 - 2276. https://doi.org/10.1109/JLT.2010.2050461

Peer reviewed version

Link to published version (if available):
10.1109/JLT.2010.2050461

Link to publication record in Explore Bristol Research
PDF-document

University of Bristol - Explore Bristol Research
General rights

This document is made available in accordance with publisher policies. Please cite only the published version using the reference above. Full terms of use are available:
http://www.bristol.ac.uk/red/research-policy/pure/user-guides/ebr-terms/

# Wireless Hybrid Mode Locked Lasers for Next Generation Radio-Over-Fiber Systems

Bilal A. Khawaja, *Student Member, IEEE*, and Martin J. Cryan, *Senior Member, IEEE*

***Abstract*—This paper demonstrates a novel technique to wirelessly injection lock a state-of-the-art 40 GHz mode locked laser and shows baseband data transmission using such a technique. This allows mode locked lasers to be used as millimeter wave modulated data sources for next generation Radio-over-Fiber systems. Binary phase shift keying data transmission rates of up to 22 Mb/s have been demonstrated for a short wireless range of 10 cm. These devices can also be used as millimeter wave phase shifters for advanced antenna beam steering systems.**

***Index Terms*—Beam steering systems, binary phase shift keying, millimeter wave, mode locked lasers, phase shifters, radio-over-fiber, wireless injection locking.**

## I. Introduction

THE demand for high speed data transmission has increased dramatically over the past few years through the evolution of wireless communications networks. To meet these requirements the millimeter-wave (mm-wave) frequency bands are becoming attractive because they offer large transmission bandwidths and also overcome the problem of spectral congestion at lower frequency ranges [1], [2]. For example, there are recently released standards for consumer based systems for the distribution of high definition TV signals around the home operating at 4 Gb/s for a wireless range of 10 m with a 60 GHz carrier [3]. To deliver similar data rates at 60 GHz in an in-building or campus wide scenario leads to hundreds of antenna deployments which results in major challenges for the current wired infrastructure. It has long been recognised that Radio-over-Fiber (RoF) links could play an important role in such systems when high-frequency wireless signals need to be distributed over many 100's of meters. The use of RoF techniques can result in a simplified overall system design since both RF carrier generation and data modulation can be done at a central base station [4]–[8].

For 60 GHz RoF systems to be feasible, cost will be a very important factor and the main issue for RoF solutions is the cost of modulating a laser at 60 GHz. An alternate solution would be the direct modulation of a laser [9] at 4 Gb/s for high speed data transmission over fiber but this would still require a 60 GHz local oscillator at the remote end for data up/down conversion using mixers which could increase the cost significantly. Traditionally, modulation at 60 GHz would be done with an expensive electro-optic modulator (EOM) [2] although more recently electro-absorption modulators have also been explored [10]. Up to now, several EOM based methods for mm-wave signal generation and data modulation using Mach–Zehnder modulator (MZM) have been proposed [2], [11]–[16]. Among these methods, double sideband (DSB) modulation schemes have a critical drawback caused by chromatic dispersion [11]. Whereas single sideband (SSB) modulation schemes [12], [13] which overcome the dispersion issue tend to have low signal-to-noise (SNR) characteristics. Other possible schemes include optical carrier suppression and optical phase modulation with optical filtering [14]–[16]. These have been applied to many RoF systems for better SNR characteristics of the generated mm-wave signals. Other techniques to generate mm-wave signals using semiconductor photonic devices have also been explored; some of the important ones are two-mode locked Fabry–Perot (FP) slave lasers [17], dual parallel injection locked FP laser [18] and an optical heterodyne technique using two single mode lasers [19]. In the optical heterodyne technique, two single-mode lasers beat together to generate a mm-wave signal at their optical frequency difference in a fast photodiode (PD).

One interesting, potentially low cost, solution is the use of mode locked lasers (MLLs) that can be designed to operate at mm-wave pulse repetition frequencies [20]. MLLs are a very attractive solution for number of applications including optical clock extraction, optical time division multiplexing, packet switching, RoF systems and microwave/mm-wave signal generation [4], [20]–[22]. Commercially available passive/hybrid MLLs are selected for this purpose because they offer high stability [20] and good phase noise performance [21]. Typically passive MLLs are fabricated from a standard FP laser which is modified to include a short saturable absorber (SA) section within the cavity. When the SA section is reversed biased, longitudinal modes within the cavity become phase locked. This results in the pulsed emission of light with a repetition frequency determined by the cavity round trip time. For typical device lengths around 1 mm this results in mm-wave repetition frequencies and thus in combination with high speed PDs can be used as mm-wave wave sources. It is well known that when a continuous wave RF signal is injected into the MLL cavity, close to its free running frequency, the MLL output signal synchronizes itself to the external signal. This condition is known as hybrid mode-locking. Such hybrid MLLs can also be used as mm-wave phase shifters under RF injection locking

Manuscript received October 28, 2009; revised January 28, 2010, March 25, 2010, April 26, 2010; accepted May 05, 2010. Date of publication May 24, 2010; date of current version August 02, 2010. The Ph.D. work of B. A. Khawaja was supported in part by the National University of Science and Technology (NUST), Islamabad, Pakistan. This work was supported in part by the Department of Electrical and Electronic Engineering, University of Bristol, U.K.

The authors are with the Photonics Research Group, Department of Electrical and Electronic Engineering, University of Bristol, Bristol, BS8 1UB, U.K. (e-mail: Bilal.Khawaja@bristol.ac.uk; m.cryan@bristol.ac.uk).

Digital Object Identifier 10.1109/JLT.2010.2050461

0733-8724/$26.00 © 2010 IEEE

[23], this shows their potential to be used in next generation smart antenna beam steering systems for WLANs. It has also been shown that in hybrid MLLs if the RF injected signal is itself modulated with baseband data, this data is imposed on the optical carrier such that it can be demodulated after a high speed PD. The first examples of this were shown sometime ago [24], [25]. In [24] 50 Mb/s differential phase-shift keying (DPSK) data transmission was demonstrated over a few meters of fiber at a 45 GHz carrier frequency. In [25] subcarrier transmission of two 2.5 Mb/s binary phase shift keying (BPSK) channels was demonstrated over 400 m of single mode fiber (SMF).

An alternate data transmission approach is the use of MLLs with EOMs. Here, MLLs running under the hybrid mode-locking condition are used with an external EOM for high speed data transmission. Ahmed *et al.* [4] showed that a 37 GHz hybrid MLL with an EOM can be used to transmit multiple video channels and 255 Mb/s BPSK data simultaneously over 10 km of SMF. They also theoretically proved that the use of hybrid MLLs as a mm-wave optical carrier source solves the problem of chromatic dispersion in SMF links operating at the link lengths of $>50$ km. Quite recently, 240 GHz [26] ultra broadband RoF transmission was achieved using an active MLL and an EOM and baseband data transmission of 3 Gb/s was demonstrated over 1 km of SMF. However, it is felt that the use of EOMs will not produce a sufficiently low cost solution for wide spread commercial deployment.

Therefore, this paper focuses on the modulator-free technique introduced in [24], [25] and explores the possibility of integrating a planar antenna along side the MLL to produce highly integrated low cost modules. This approach is being explored at lower frequencies and is termed as photonic active integrated antenna [27], [28]. The advantage in this case is that in the mm-wave bands antennas become sufficiently small such that they could be integrated directly on the same semiconductor substrate as the laser. This has already been implemented for high speed PDs [29], but to the author's knowledge has not been explored for lasers. Such fully monolithic photonic active integrated antenna chips could radically reduce the costs of mm-wave RoF systems and could lead to the widespread adoption of this technology. A typical mm-wave RoF system architecture is shown in Fig. 1 where a central base station feeds a fiber network which delivers mm-wave modulated light to low cost remote antenna units. An important advantage of using a RoF system is that long ($\sim$kms) link lengths can be implemented meaning large building and campus wide networks can be covered with one central base station. The advantages of using fibre over copper based approaches are that the link loss is essentially independent of the carrier frequency and the loss is so low ($\sim$0.2 dB/km) that the system design is virtually independent of link length. Dispersion induced fading [30] can be an issue with longer RoF links, but for links in the few km range it is not that critical. In the implementation proposed here the remote antenna units will contain high speed PDs for the downlink and wireless hybrid MLLs for the uplink. The MLLs can also be used for mm-wave signal generation and modulation at the central base station for downlink data transmission. Fig. 1 also shows the use of steerable beams which could in principle be implemented using the phase shifting ability of injection locked systems [23]. However, to implement beam steering multiple laser chips and optical combiners would be required, this will be studied in future work. The paper is organized as follows: Section II shows 40 GHz MLL characterization results, including RF injection locking and phase shifting. In Section III, a 40 GHz patch antenna design and wireless hybrid mode-locking results are presented. Section IV presents baseband data transmission results using both hybrid MLL and wireless hybrid MLLs and Section V draws conclusions.

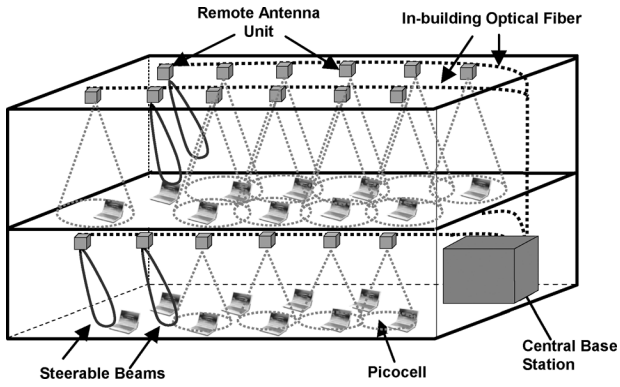


Fig. 1. Schematic of mm-wave RoF system architecture.

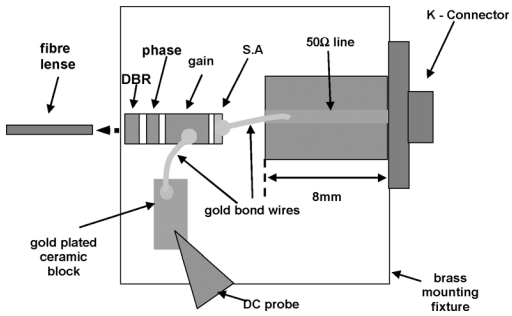


Fig. 2. Schematic of MLL mounting configuration.

## II. 40 GHz Mode-Locked Laser Characterization

### A. Passive Mode-Locking and Tuning Range

The state-of-the-art 1550 nm monolithic InP-based multiple quantum-well devices have been used for the measurements. They possess a distributed bragg reflector, an integrated saturable absorber (SA), gain and phase sections as shown schematically in Fig. 2. The multi-section MLL devices were supplied by HHI, Berlin [20] having a total device length of 1080 $\mu$m which produces an output pulse repetition frequency of around 40 GHz. Fig. 2 also shows the device mounting configuration. Two MLL devices, MLL-A2 and MLL-A3 were used for the measurements. A brass fixture was used to mount the MLL for testing. The SA section was connected using a gold bond wire and a 50 $\Omega$ transmission line with a K-connector to apply both RF power and reverse bias to the SA section for hybrid mode-locking. A separate gold plated ceramic block was connected to the gain section of the MLL using a bond wire and

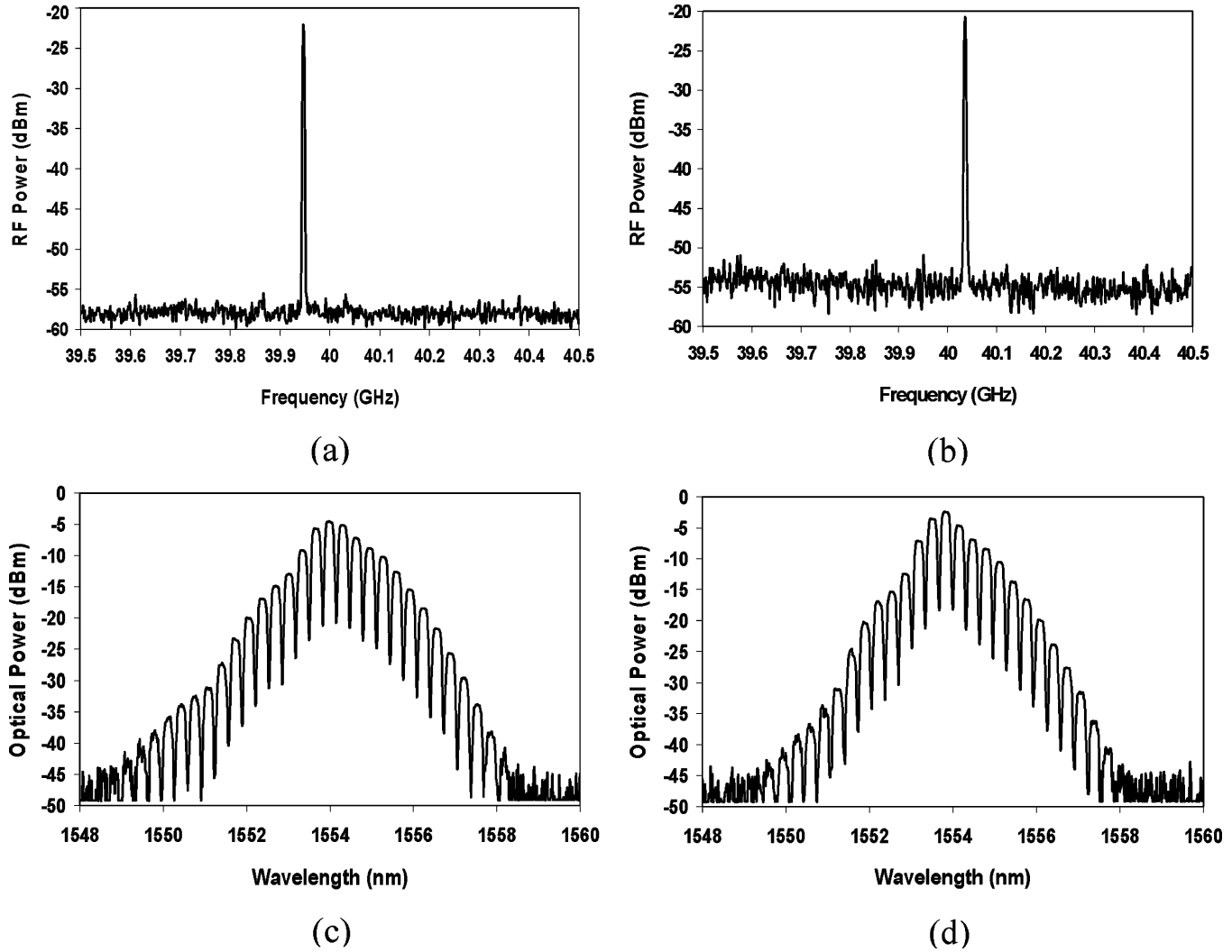


Fig. 3. (a), (b) Measured millimetre-wave passive mode-locking RF spectra ($\mathrm{Span} = 1$ GHz, Res $\mathrm{BW} = 3$ MHz) and (c), (d) Optical Spectra at $I_g = 110$ mA, $V_{\mathrm{sa}} = -1.0$ V for MLL-A2 and MLL-A3 respectively.

a DC probe was used to apply forward bias to the gain section. It should be noted that phase and distributed bragg reflector sections were unbiased for all the MLL measurements.

Both MLL-A2 and MLL-A3 have excellent optical output powers of ~7.5 mW and 8.5 mW respectively. These were measured into a single mode fiber lens at 110 mA gain section current and operating temperature of 15°C. Passive mode-locking of the MLLs was then performed and the mm-wave spectrum was observed using an Agilent 50 GHz (E4448A) spectrum analyzer and a high speed $\mathrm{U}^2$ t Photonics 50 GHz PD. Fig. 3(a), (b) shows the passive mode locked RF spectra and Fig. 3(c), (d) shows optical spectra respectively. The gain and SA sections of the MLLs were biased at 110 mA and $V_{\mathrm{sa}} = -1.0$ V for MLL-A2 and MLL-A3 respectively. The slight differences in the spectra in terms of passive mode locked frequency, noise floor and power level, reflect the device-to-device repeatability for this type of semiconductor device. The free running frequency of the MLL can be controlled by the SA voltage and gain section bias and has a range of 446.7 MHz [23] and 466.6 MHz for MLL-A2 and MLL-A3 respectively.

### B. MLL Injection Locking

Hybrid mode-locking of the MLL can be achieved by injecting a continuous wave external RF signal into the MLL cavity close to its passively mode locked frequency. The MLL repetition rate is then controlled by the applied external RF signal over a range over frequencies known as the locking range. Hybrid mode-locking of these MLLs has been extensively characterized in [20] and recently, a novel approach has been presented by injection locking the MLL using a vector network analyzer (VNA) [23] which exploits the phase locked nature of a VNA. Fig. 4 shows the measurement setup.

In the setup, port 1 of a VNA is used to input a mm-wave signal into the SA section to obtain injection locking. Light is coupled out of the laser using a single-mode fiber lense and into a high speed PD and back into port 2 of the VNA. The gain section was biased at 110 mA and the SA section was biased at range of voltages from $-0.5$ V to $-1.5$ V. The maximum VNA output power is $-6$ dBm which is quite low and to overcome this, a $+23$ dB gain SHF (804TL) mm-wave high power amplifier (HPA) was used to increase the amount of RF input power

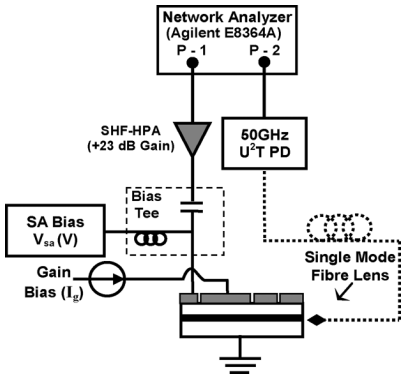


Fig. 4. MLL Injection Locking measurement setup using mm-wave amplifier and VNA.

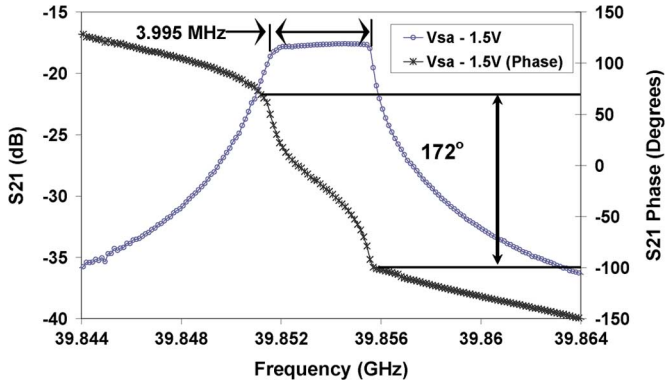


Fig. 5. Zoom-in on $S_{21}$ amplitude response showing plateau across locking range and its relative phase shift of 172° measured using MLL-A2.

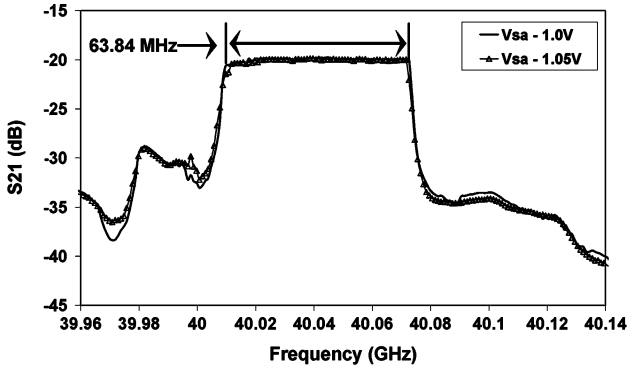


Fig. 6. Zoom-in on $S_{21}$ amplitude response showing plateau across locking range of 63.84 MHz for $V_{\rm sa} = -1.0$ V and $-1.05$ V measured using MLL-A3.

to the MLL for wider locking ranges. An RF power of $+12.6$ dBm was injected into the laser fixture after the HPA, bias-t and the V-K connectors. The loss from connector to SA section is estimated from separate fixture measurements to be $-1.6$ dB, thus the input power to the SA section is estimated to be $+11$ dBm. The VNA measures the link gain $(S_{21})$ of the system. The locking range can be observed as a flat "plateau" in the $S_{21}$ amplitude response as shown in Fig. 6 where the swept frequency of the VNA is locking the free running frequency of the MLL.

This technique not only allows a straight forward characterization of mm-wave injection locking between MLL and VNA but also provides an easy characterization of mm-wave phase shift induced due to RF injection locking of the two systems. According to classical electronic injection-locked oscillator (ILO) theory [31]–[33], the phase of an ILO will shift by 180° ($\pi/2$ to $-\pi/2$) as the injected signal is tuned across the oscillator's locking range, as given by the formula in (1)

$$\theta(\omega_1) = \sin^{-1}\left(\frac{\omega_0 - \omega_1}{\Delta\omega_L}\right) \tag{1}$$

where $\omega_0$ and $\omega_1$ are the output and injected frequencies respectively and $\Delta\omega_L$ is the locking range of the ILO.

Fig. 5 below shows MLL-A2 injection locked measured $S_{21}$ amplitude and phase response and it can be seen that an overall phase shift of 172° is observed. It is important to note here that the injection locked MLL presented in [23] and in this paper is behaving like an electronic ILO, but in reality it is an optoelectronic system which is fundamentally different and more complex than an electronic ILO system.

The widest locking range obtained is 63.84 MHz from MLL-A3 as shown in Fig. 6. This is the highest locking range achieved so far from the VNA based injection locking technique introduced in [23]. However, these lasers have not been optimized for wide locking range and other MLL configurations have shown much wider locking ranges, upto 500 MHz–2 GHz [20].

It is also well known that the locking range is dependent on the amount of injected power with greater input power producing increased locking ranges [31]–[33], as given by the formula in (2)

$$\Delta\omega_L \propto \sqrt{P_{\rm inj}} \tag{2}$$

where $P_{\rm inj}$ is the injected RF power to the MLL.

The effect of change in SA injection power $(P_{\rm inj})$ on the locking range is now studied. To this end, the MLL-A2 is again injection locked using a mm-wave ($+14$ dB gain) amplifier using similar setup configuration shown in Fig. 4. The gain and SA bias were fixed at $+110$ mA and $V_{\rm sa} = -1.5$ V respectively. The effect of changing $P_{\rm inj}$ on the locking range is shown in Fig. 7. It can be seen that a locking range of 3.895 MHz is observed for $P_{\rm inj} = -1.7$ dBm and as the injection power level decreases the locking range decreases as expected from (2). Fig. 7 also shows that the link gain level and centre frequency of the locking range are dependent on the injected power, this is most likely due the highly non-linear nature of the injection locked system.

The locking range can now be plotted against square root of the injected power in order to understand whether the MLL system is behaving like an electronic ILO.

The MLL locking range is extracted from Fig. 7 for each SA injection power. It can be seen in Fig. 8 that the locking range is reasonably linear with respect to the $\sqrt{P_{\rm inj}}$ from 0.35 $\sqrt{(\rm mW)}$ to 0.7 $\sqrt{(\rm mW)}$. Outside this range the data no longer agrees with the linear fit given in (2) and this is believed to be due to complex nature of the locking process here.

## III. Wireless Hybrid Mode-Locked Laser

Wireless hybrid mode-locking is a new concept where a MLL is combined with a planar antenna such that it can be wirelessly

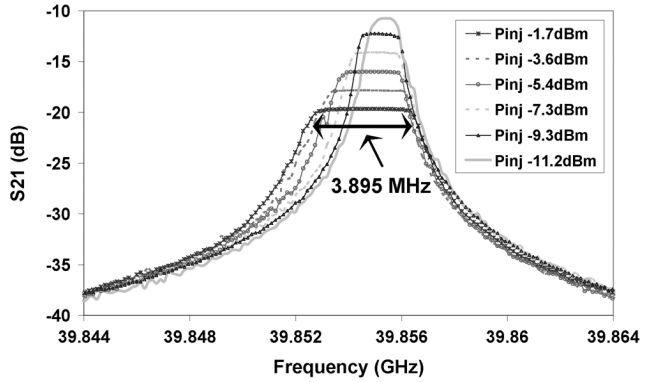


Fig. 7. Zoom-in on $S_{21}$ amplitude response showing locking range for different SA injection powers measured using MLL-A2.

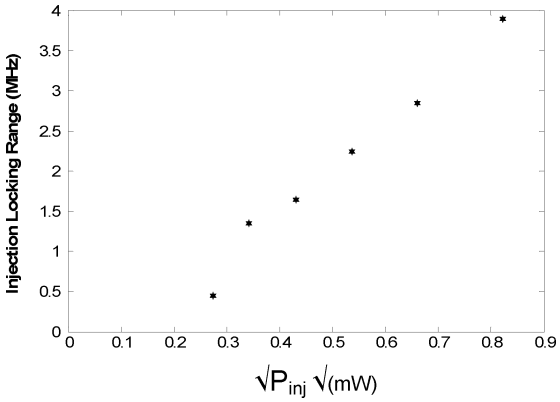


Fig. 8. Shows the dependence of Injection locking range on square root of locking signal power.

injection locked for baseband data transmission. This technique has been recently introduced and demonstrated in [34], [35] and is a first step towards the full monolithic integration of MLLs with antennas and amplifiers. There are issues with the integration of amplifiers in this case, but there are a number of novel schemes that have been suggested [36].

### *A. Millimeter-Wave Antenna Characterization for Wireless Injection Locking*

This section shows MLL wireless injection locking range results using a waveguide-to-coax horn antenna at the transmit end and a patch antenna at the receiving end. A standard rectangular patch antenna is designed using the Agilent Advanced Design System Momentum simulator. RT/Duroid high frequency glass microfibre substrate ($\varepsilon_r = 2.33$ and $\text{thickness} = 0.254$ mm) is chosen for the antenna design because of its low loss and good working characteristics at mm-wave frequencies. The patch antenna was mounted on a brass fixture and has dimensions of 1.59 mm $\times$ 2.34 mm. Both horn and patch antennas were designed to operate around 40 GHz. The horn antenna is used at the transmit end because in future smart antenna beam steering systems, antenna arrays can be used in small picocells at the remote antenna unit to locate users. Antennas arrays will have high gain which is similar to the gain of a typical horn antenna.

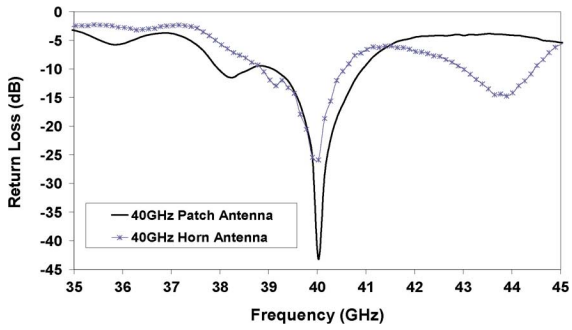


Fig. 9. Measured return loss of 40 GHz horn and patch antennas.

The horn antenna used for the measurement has a gain of 7.66 dBi measured seperately from the current setup.

The return loss of the two antennas was measured using the VNA as shown in Fig. 9. The antennas have a bandwidth of $>1.2$ GHz which would support multi-gigabit communications. The path loss is typically quite high at mm-wave frequencies even for short distances and to this end the $S_{21}$ measurement was done between the horn and patch antenna. The measured path loss at 40 GHz is $-37.8$ dB, when the distance between the two antennas was 20 cm. This path loss implies that more amplification is required at 40 GHz to wirelessly injection lock the MLL.

### *B. MLL and Horn to Patch Antenna Measurement Results*

The wireless injection locking measurement configuration of MLL-A2 is performed using a horn antenna at the tranmitting end and a patch antenna at the receiving end. The patch antenna is then connected to the SA section of the MLL using a high frequency V-type coaxial cable. The set up is shown schematically in Fig. 10. The maximum output power from the VNA is $-6$ dBm. Port 1 of the VNA is connected to a SHF mm-wave HPA and a coaxial cable having a separately measured loss of $-2.35$ dB at 40 GHz and then to the transmitting horn antenna. The radiated signal is received at the patch antenna and fed through three mm-wave amplifiers connected in series having individual gains of $+10.3$ dB, $+14.05$ dB and $+12.9$ dB respectively. The small signal gain $(G_S)$ for these cascaded amplifiers is $\sim$37 dB but the separately measured large signal gain $(G_L)$ in this setup configuration is $\sim$18 dB. The signal is then fed to the SA section of the MLL. The optical output of the MLL is then fed through a single mode fiber lens to the PD and back into port 2 of VNA.

Wireless injection locking is observed from the $S_{21}$ amplitude response as shown in Fig. 11. This figure also shows the phase shifting operation that can be achieved by varying the bias conditions of the MLL as outlined previously [23], [34], [35], [37]. A relative normalized phase shift of $>150$ degrees is then measured in this case.

It is also important to observe the radiation patterns of the antenna which can be measured directly by rotation of the receiving antenna. Fig. 12 shows the results at different $V_{\text{sa}}$ values of $-1.05$ V to $-1.15$ V. It can be seen that very consistent patterns are being obtained at the different $V_{\text{sa}}$ values implying that good beamforming operation will be possible.

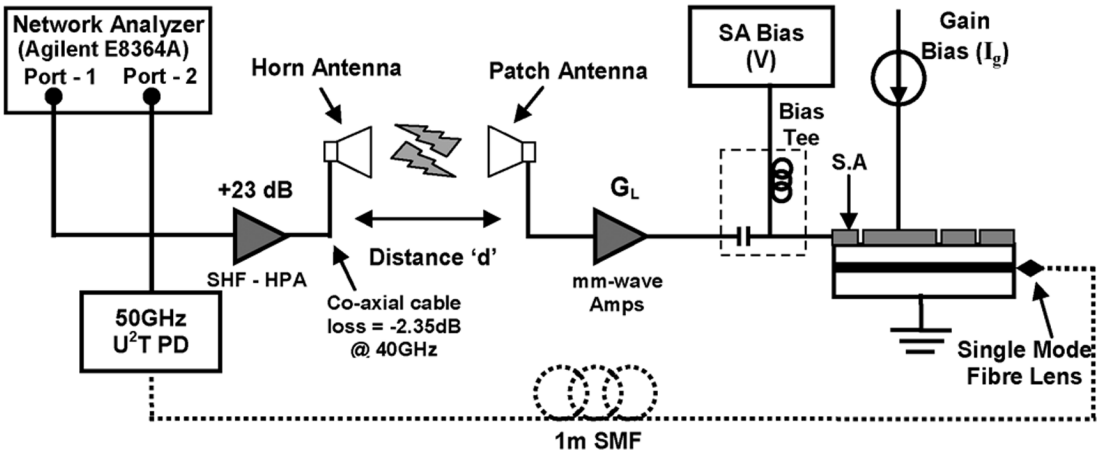


Fig. 10. MLL measurement setup using mm-wave horn, patch antenna and amplifiers for phase shift measurements. Distance between two $\mathrm{Antennas} = 20$ cm.

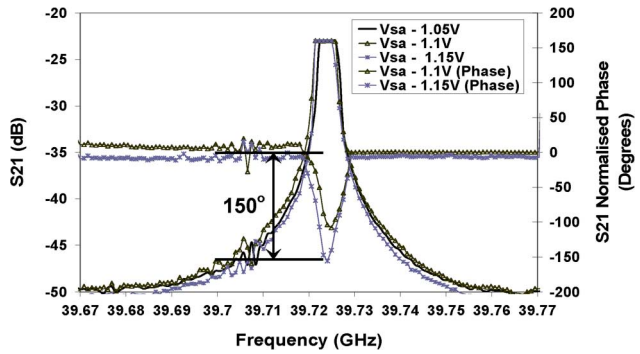


Fig. 11. Measured magnitude and phase of $S_{21}$ at different SA reverse bias values (Phases are normalized to $V_{\mathrm{sa}} = -1.05$ V) for MLL-A2, Distance between horn and patch $\mathrm{Antennas} = 20$ cm.

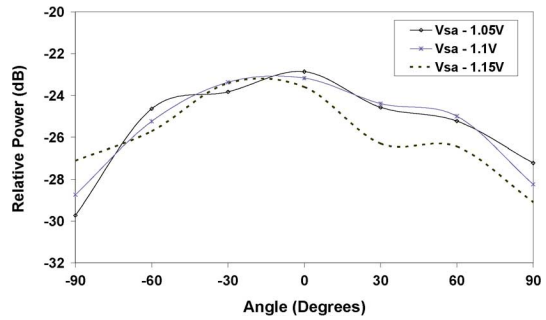


Fig. 12. Measured radiation pattern between the horn and patch antennas at $V_{\mathrm{sa}} = -1.05$ V to $-1.15$ V for MLL-A2, Distance between two $\mathrm{Antennas} = 20$ cm.

## IV. Hybrid Mode-Locked Laser as Millimeter Wave Modulated Data Source

A number of techniques for the generation, modulation, and distribution of mm-wave modulated optical carriers for RoF systems have been described in the literature [2], [4], [6]–[14], [17]–[22]. The most common technique is the use of expensive external MZM [2], [11]–[16]. Although, quite recently a medium-cost approach has been demonstrated for Gb/s data transmission using a directly modulated un-cooled distributed feedback laser and an optically generated 40 GHz local oscillator source [38]. This section shows how a MLL can be used as mm-wave modulated data source and discusses how the MLL locking range is related to the maximum baseband data that can be transmitted. This section then presents what is believed to be the first demonstration of BPSK wireless data transmission using the Wireless hybrid mode-locking technique.

### A. BPSK Data Transmission Over a MLL-RoF Link

MLL-A3 is biased at a gain section current of 110 mA, with an optical output power of ~8.5 mW, and $V_{\mathrm{sa}} = -1.1$ V is used for the data transmission. The setup diagram is shown in Fig. 13, where a 2 V peak-to-peak pseudorandom $(2^7 - 1)$ non-return-to-zero (NRZ) bit sequence is generated from an Anritsu ME522A pattern generator. The BPSK data is upconverted to 40 GHz using a Hittite (HMC-560) GaAs MMIC mixer. A 40 GHz Wiltron sweeper is used as a local oscillator source to drive the up and down conversion mixer local oscillator ports using a RF splitter. The sweeper output power is $+6$ dBm which after the coaxial cable and splitter is $-3$ dBm which is too low to drive the mixer local oscillator port. Thus, a mm-wave amplifier is used at each side for both up and down conversion as shown in Fig. 13. The upconverted data is then amplified using a SHF mm-wave HPA and injected into the SA section of the MLL. It is important to note here that the amplification used here is similar to the one shown in Fig. 4 which gave a wide locking range of 63.84 MHz as shown in Fig. 6.

The light at the output of MLL is coupled into the 1 m single mode fiber lens and fed through the polarization controller and then into the 50 GHz PD. The mm-wave modulated signal from the PD was then amplified using a $+14.5$ dB gain amplifier and fed to the RF port of mixer-2 for down conversion. The down converted data at the IF port was then amplified using a $+30$ dB gain Westminster wideband (SN60801) amplifier. After a low pass filter, the data was fed into a Lecroy Wave Pro ($760Z_i$) 6 GHz oscilloscope to observe the detected eye-diagrams in the time domain as shown in Fig. 14(a), (b).

The maximum data rate achieved using this technique is 56 Mb/s as shown in Fig. 6. It can be seen that a good eye opening is observed up to data rates of 56 Mb/s which shows successful data transmission.

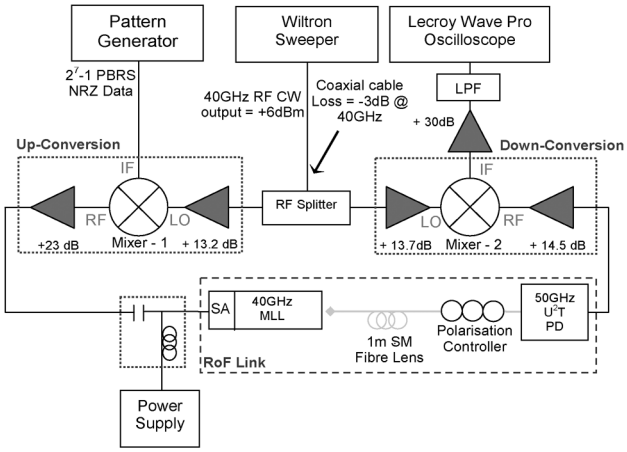


Fig. 13. MLL measurement setup for BPSK data transmission.

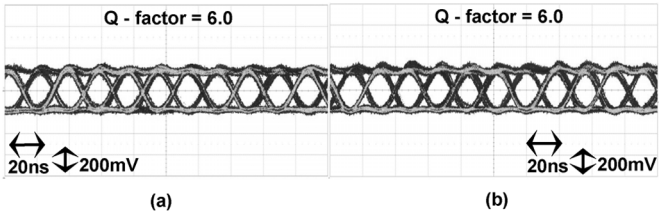


Fig. 14. Downconverted NRZ data eye diagrams for the data rates of (a) 54 Mb/s NRZ data eye diagram and (b) 56 Mb/s over MLL-RoF Link.

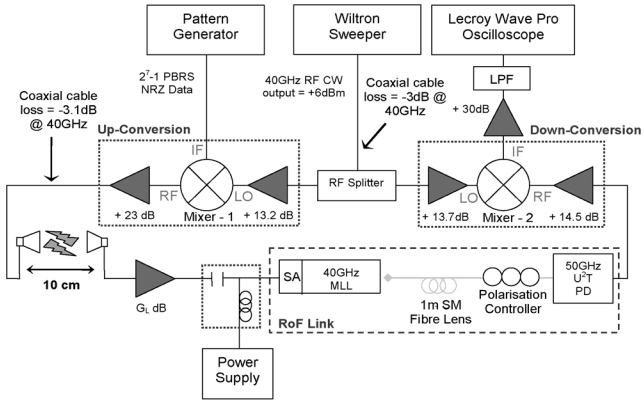


Fig. 15. MLL wireless injection locking and BPSK data transmission setup using horn to patch antenna. Distance between $\mathrm{antennas} = 10$ cm.

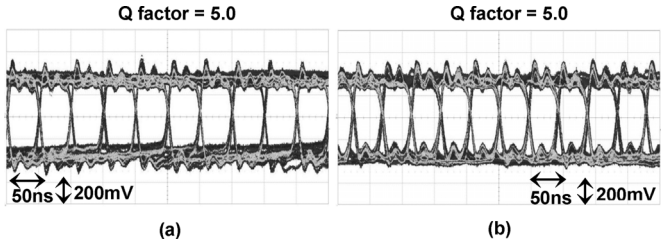


Fig. 16. Downconverted NRZ data eye diagrams for the data rates of (a) 20 Mb/s NRZ data eye diagram and (b) 22 Mb/s NRZ data eye diagram using horn to patch antenna and MLL for BPSK data transmission using wireless injection locking technique, distance between $\mathrm{antennas} = 10$ cm.

The Quality factors $(Q)$ of the eye diagrams are then measured. The $Q$-factor predicts the probability of bit errors by measuring the received signal strength and noise level rather than by counting actual errors [38]. It can be seen from Fig. 13 that for the maximum data rates of 54 and 56 Mb/s, the measured $Q$-factor is 6, which corresponds to a *BER* of $10^{-9}$ [39]. It is important to note that this is the highest achieved BPSK data rate using the MLL based data transmission technique introduced in [35], [37].

### B. BPSK Wireless Data Transmission

This section presents the results of NRZ-BPSK data transmission using the wireless hybrid mode-locking technique. Fig. 15 shows the measurement setup which is similar to the one shown in Fig. 13. The main difference is that a wireless link of distance 10 cm between a horn and patch antenna has been added.

To overcome the extra path loss, measured to be $-29.8$ dB at 40 GHz, three mm-wave amplifiers are added after the patch antenna. A similar data up and down conversion approach is used here. The upconverted BPSK data at 40 GHz is amplified by a SHF mm-wave HPA and fed to the horn antenna using a coaxial cable with a loss of $-3.1$ dB at 40 GHz. The patch antenna receives the signal which is then amplified using three cascaded mm-wave amplifiers having $G_L = \sim 18$ dB gain. The amplified signal is fed to the SA section of the MLL-A2 which was biased at gain section current of 110 mA and $V_{\mathrm{sa}} = -1.18$ V. After the PD and down conversion mixer the recovered eye diagrams are obtained and shown in Fig. 16(a), (b).

Good eye opening and measured $Q$-factor of 5 is observed in Fig. 16 which shows the successful error-free wireless BPSK data transmission up to 22 Mb/s. The reduced data rate here is related to the reduced locking range in this case. These results show the ability of a MLL to be used as mm-wave modulated data source using the wireless injection locking technique.

### C. Discussion

This paper has shown a maximum data rate of 56 Mb/s, it is important to understand what limits this. From previous work [35] a maximum data rate of 26 Mb/s was obtained. Both of these results were obtained with the same type of MLL chip and the main difference between the cases was that here a maximum locking range of 63.84 MHz is obtained where as in [35] only 30.46 MHz was achieved. The reason for this difference in locking range is due to the amount of injected power. As shown in (2) locking range is strongly related to injected power and here by careful reduction of losses and increase in amplification the injected power as been significantly increased, resulting in increased locking range. These results together suggest that there is strong relationship between locking range and maximum data rate, with a doubling in locking range resulting in a doubling of data rate. The locking phenomenon here is however, a complex one and other factors related to carrier dynamics in the MLL cavity could be playing an important role as well. As discussed previously, these MLL devices have not been optimized for wide locking ranges and other laser configurations integrated with electro-absorption modulators [20], [40] have shown much wider locking ranges. A reasonable locking range of 500 MHz [20] for hybrid mode locking has been demonstrated. On the other hand, Arahira *et al.* [40] have published a

much larger locking range of 1.9 GHz for 40-GHz/1.55 $\mu$m active MLL. However, the 1.9 GHz locking range devices are not commercially available. It is however believed that specifically designed MLL devices integrated with SA sections can produce wider locking ranges and hence higher modulation bandwidths.

This paper has concentrated on device characterisation and wireless transmission of data using short lengths of SMF $\sim$ 2 m. Other workers have shown similar techniques [24], [41] and have included longer fibre lengths of between 50–400 m of SMF. In these injection locked modulation schemes there will be a number of effects which will limit the fibre range for a given data rate and mm-wave carrier frequency including sideband cancellation [11] and the laser spectral width. However, the technique has been shown to work over 400 m of SMF [24] and it is felt that for the envisaged applications of in-building/campus wide pico-cellular systems it is likely that these fibre ranges will be sufficient.

The wireless data transmission results using MLLs shown here are for a short range of 10 cm, realistic applications would be in the range 5–10 m range. It should be noted that the mm-wave output power at the PD does not have a simple dependence on the power injected in to the SA section. Thus, link gain calculations are more complex in this MLL-injection locked system. This is highlighted in Fig. 7 where the link gain increases with decreasing input power to the SA section. It is expected that specifically designed MLLs could have a much wider locking range which could enable high data rate communications in the 5–10 m range. The path loss for 5 m is 64.88 dB at 40 GHz, an increase of 35.08 dB over the 10 cm case shown here. It is felt that this extra loss could be compensated by increased amplification in the system and also by the use of beamforming techniques to produce high gain beams for the uplink. For example in [41] a range of 10 m was achieved by using high gain amplifiers and horm antennas. Interestingly, here it also possible to use a semiconductor optical amplifier to boost the output optical power of the MLL. If this device was monolithically integrated with the MLL, the cost implications would not be that great. One further solution would be the monolithic integration of a MLL with a RF amplifier and antenna, this will be explored in the future work.

## V. Conclusion

This paper has shown what is believed to be the first example of simultaneous wireless injection locking of a MLL and 22 Mb/s NRZ BPSK data transmission using a wireless connection to the SA section. It describes the factors which limit the maximum data rate which can be achieved using MLL injection locking and a maximum data rate of 56 Mb/s is achieved for a locking range of 63.84 MHz. This paper has shown a modular integration approach using K-connector fixtures. Future work will combine the MLL, amplifiers and planar antenna on the same mount to create a very compact module. This is a stepping stone to full monolithic integration of MLLs with antennas which could dramatically reduce the costs of such radio-over-fiber systems.

## References


[1] P. F. M. Smulders, "60 GHz radio: Prospects and future directions," in *Proc. Symp. IEEE Benelux Chapter on Communications and Vehicular Technol.*, Eindhoven, 2003, pp. 1–8.

[2] R. W. Ridgway and D. W. Nippa, "Generation and modulation of a 94-GHz signal using electro-optic modulators," *IEEE Photonics Tech. Lett.*, vol. 20, no. 8, pp. 653–655, Apr. 2008.

[3] WiHD [Online]. Available: http://www.wirelesshd.org

[4] Z. Ahmed *et al.*, "37-GHz fiber-wireless system for distribution of broadband signals," *IEEE Trans. Microw. Theory Tech.*, vol. 45, no. 8, pp. 1431–1435, Aug. 1997.

[5] C. H. Cox, III, *Analog Optical Links*. Cambridge, U.K.: Cambridge Univ., 2004.

[6] M. Sauer, K. Kojucharow, H. Kaluzni, D. Sommer, W. Nowak, and A. Finger, "Radio-optical system design and transmission experiments for a mobile broadband communications system at 60 GHz," *Wireless Pers. Commun.—Special Issue Radio Over Fibre-Systems, Technologies Applications*, vol. 14, no. 2, pp. 147–163, Aug. 2000.

[7] A. J. Seeds, "Microwave photonics," *IEEE Trans. Microw. Theory Tech.*, vol. 50, no. 3, pp. 877–887, Mar. 2002.

[8] M. Sauer, A. Kobyakov, and J. George, "Radio over fiber for picocellular network architectures," *J. Lightw. Tech.*, vol. 25, no. 11, pp. 3301–3319, Nov. 2007.

[9] J. K. White, C. Blaauw, P. Firth, and P. Aukland, "85°C investigation of uncooled 10-Gb/s directly modulated InGaAsP RWG GC-DFB lasers," *IEEE Photonics Technol. Lett.*, vol. 13, no. 8, pp. 773–775, Aug. 2001.

[10] K.-S. Choi *et al.*, "System-on-packaging with electroabsorption modulator for a 60-GHz band radio-over-fiber link," *IEEE Trans. Adv. Packaging*, vol. 31, no. 1, pp. 63–169, Feb. 2008.

[11] G. H. Smith, D. Novak, and Z. Ahmed, "Overcoming chromatic-dispersion effects in fiber-wireless systems incorporating external modulators," *IEEE Trans. Microw. Theory Tech.*, vol. 45, no. 8, pp. 1410–1415, Aug. 1997.

[12] K. Yonenaga and N. Takachio, "A fiber chromatic dispersion compensation technique with an optical SSB transmission in optical homodyne detection systems," *IEEE Photon. Technol. Lett.*, vol. 5, no. 8, pp. 949–951, Aug. 1993.

[13] M. Attygalle, C. Lin, G. J. Pendock, A. Nirmalathas, and G. Edvell, "Transmission improvement in fiber wireless links using fiber Bragg gratings," *IEEE Photon. Tech. Lett.*, vol. 17, no. 1, pp. 190–192, 2005.

[14] J. Li, T.-G. Ning, L. Pei, and C. H. Qi, "Scheme for a high-capacity 60 GHz radio-over-fiber transmission system," *IEEE/OSA J. Opt. Comm. Netw.*, vol. 1, no. 4, pp. 324–330, Sep. 2009.

[15] G. Qi, J. Yao, J. Seregelyi, S. Paquet, and C. Bélisle, "Optical generation and distribution of continuously tunable millimeter-wave signals using an optical phase modulator," *J. Lightw. Technol.*, vol. 23, no. 9, pp. 2687–2694, Sep. 2005.

[16] P. Shen, J. James, N. J. Gomes, P. G. Huggard, and B. N. Ellison, "Low-cost, continuously tunable, millimeter-wave photonic LO generation using optical phase modulation and DWDM filters," *IEEE Photon. Technol. Lett.*, vol. 20, no. 23, pp. 1986–1988, Dec. 2008.

[17] T. Taniguchi *et al.*, "Full-duplex 1.0 Gbit/s data transmission over 60 GHz radio-on-fiber access system based on the loop-back optical heterodyne technique," *J. Lightw. Technol.*, vol. 26, no. 13, pp. 1765–1776, Jul. 2008.

[18] M.-K. Hong, Y.-Y. Won, and S.-K. Han, "Gigabit optical access link for simultaneous wired and wireless signal transmission based on dual parallel injection-locked Fabry-Pérot laser diodes," *J. Lightw. Technol.*, vol. 26, no. 15, pp. 2725–2731, Aug. 2008.

[19] L. Noel, D. Wake, D. G. Moodie, D. D. Marcenac, L. D. Westbrook, and D. Nesset, "Novel techniques for high-capacity 60-GHz fiber-radio transmission systems," *IEEE Trans. Microw. Theory Tech.*, vol. 45, no. 8, pp. 1416–1423, Aug. 1997.

[20] R. Kaiser and B. Huttl, "Monolithic 40-GHz mode-locked MQW DBR lasers for high-speed optical communication systems," *IEEE J. Sel. Topics In Quantum Elec*, vol. 13, no. 1, pp. 125–135, Jan./Feb. 2007.

[21] B. Huettl, R. Kaiser, M. Kroh, C. Schubert, G. Jacumeit, and H. Heidrich, "Optical 40 GHz pulse-source module based on a monolithically integrated mode locked DBR laser," *SPIE Proc., Optoelec. Materials and Devices for Opt. Comms.*, vol. 6020, pp. 479–487, 2005.

[22] S. Arahira and Y. Ogawa, "Polarization-insensitive all-optical 160-Gb/s clock recovery with a monolithic passively mode-locked laser diode in polarization-diversity configuration," *IEEE J. Quantum Electron.*, vol. 43, no. 12, pp. 1204–1210, Dec. 2007.

[23] B. A. Khawaja and M. J. Cryan, "Study of millimeter wave phase shift in 40 GHz hybrid mode locked lasers," *IEEE Microw. Wireless Comp. Lett.*, vol. 19, no. 3, pp. 182–184, Mar. 2009.
[24] J. B. Georges *et al.*, "Optical transmission of narrowband millimeter-wave signals by resonant modulation of monolithic semiconductor lasers," *IEEE Photon. Technol. Lett.*, vol. 6, no. 4, pp. 568–570, Apr. 1994.
[25] J. B. Georges, D. M. Cutrer, M.-H. Kiang, and K. Y. Lau, "Multichannel millimeter wave subcarrier transmission by resonant modulation of monolithic semiconductor lasers," *IEEE Photon. Technol. Lett*, vol. 7, no. 4, pp. 431–433, Apr. 1995.
[26] T. Ohno, F. Nakajima, T. Furuta, and H. Ito, "A 240-GHz active modelocked laser diode for ultra-broadband fiber-radio transmission systems," in *Tech. Dig. Opt. Fiber Comm. Conf.*, Mar. 2005, vol. 6, pp. 3–.
[27] V. Sittakul and M. J. Cryan, "A fully bidirectional 2.4-GHz wireless-over-fiber system using photonic active integrated antennas (PhAIAs)," *J. Lightw. Technol.*, vol. 25, no. 11, pp. 3358–3365, Nov. 2007.
[28] V. Sittakul and M. J. Cryan, "A 2.4-GHz wireless-over-fibre system using photonic active integrated antennas (PhAIAs) and lossless matching circuits," *J. Lightw. Technol.*, vol. 27, no. 14, pp. 2724–2731, Jul. 2009.
[29] A. Hirata, H. Ishii, and T. Nagatsuma, "Design and characterization of a 120-GHz millimeter-wave antenna for integrated photonic transmitters," *IEEE Trans. Microw. Theory Tech.*, vol. 49, no. 11, pp. 2157–2162, Nov. 2001.
[30] U. Gliese, S. Nørskov, and T. N. Nielsen, "Chromatic dispersion in fiber-optic microwave and millimeter-wave links," *IEEE Trans. Microw. Theory Tech.*, vol. 44, pp. 1716–1724, Oct. 1996.
[31] R. Adler, "A study of locking phenomena in oscillators," *Proc. IEEE*, vol. 61, pp. 1380–1385, Oct. 1973.
[32] A. E. Siegman, *Lasers*. Oxford, U.K.: Oxford University Press, 1986.
[33] A. Zarroug, P. S. Hall, and M. J. Cryan, "Active antenna phase control using subharmonic locking," *IEEE Electron. Lett.*, vol. 31, no. 11, pp. 842–843, May 1995.
[34] B. Khawaja, I. Djordjevic, and M. Cryan, "A millimeter wave phase shifter using a wireless hybrid mode locked laser," in *Proc. OFC*, San Diego, CA, Mar. 22–26, 2009, Paper OTuM5.
[35] B. A. Khawaja and M. J. Cryan, "A wireless hybrid mode locked laser for low cost millimetre wave radio-over-fiber systems," in *Proc. Int. Top. Meeting Microwave Photonics 2009*, Valencia, Spain, Oct. 2009, pp. 1–4.
[36] O. Wada, T. Sanada, and T. Sakurai, "Monolithic integration of an AlGaAs/GaAs DH LED with a GaAs FET driver," *IEEE Electron Dev. Lett.*, vol. 3, no. 10, pp. 305–307, Oct. 1982.
[37] B. A. Khawaja and M. J. Cryan, "A hybrid mode locked laser as millimetre wave modulated data source for radio-over-fiber systems," in *Proc. Summer Topical Meeting, 2009. LEOSST'09. IEEE/LEOS*, Newport Beach, CA, Jul. 20–22, 2009, pp. 67–68.
[38] T. Ismail, C. P. Liu, J. E. Mitchell, and A. J. Seeds, "Transmission of Gb/s DPSK millimeter-wave wireless data over fiber using low-cost uncooled devices with remote 40-GHz local oscillator delivery," *J. Lightw. Technol.*, vol. 26, no. 21, pp. 3490–3496, Nov. 2008.
[39] I. P. Kaminow and T. Li, *Optical Fiber Telecommunications IV: Systems and Impairment*. New York: Academic, 2002, pp. 174–.
[40] S. Arahira and Y. Ogawa, "40 GHz actively mode-locked distributed Bragg reflector laser diode module with an impedance-matching circuit for efficient RF signal injection," *Jpn. J. Appl. Phys.*, vol. 43, no. 4B, pp. 1960–1964, 2004.
[41] F. Lecoche, E. Tanguy, B. Charbonnier, H. Li, F. van Dijk, A. Enard, F. Blache, M. Goix, and F. Mallécot, "Transmission quality measurement of two types of 60 GHz millimeter-wave generation and distribution systems," *J. Lightw. Technol.*, vol. 27, no. 23, pp. 5469–5474, Dec. 2009.

**Bilal A. Khawaja** was born in Karachi, Pakistan, in August 1980. He received the B.Sc. (computer engineering) degree from Sir Syed University of Engineering and Technology, Karachi, Pakistan, in 2002 and the M.Sc. degree in communication engineering and signal processing from University of Plymouth, Plymouth, U.K., in 2005.

He worked as a software engineer from 2003 to 2004 in Simcon International (Pvt.) Ltd. He has been working towards the Ph.D. degree at the University of Bristol, Bristol, U.K., since 2006. His research interests are in next generation radio-over-fibre systems and mode-locked lasers.

**Martin J. Cryan** received the B.Eng. degree in electronic engineering from the University of Leeds, U.K., in 1986 and then worked in industry for five years as a microwave design engineer. In 1995 he received the Ph.D. degree from the University of Bath, U.K., for work on GaAs MMIC design.

From 1994 to 1997 he was a Researcher at the University of Birmingham, U.K., where he worked on active integrated antennas. From 1997 to 1999 he was a European Union Training and Mobility of Researchers research fellow working at the University of Perugia, Italy on the design and simulation of quasi-optical multipliers using the Lumped—Element FDTD method. From 2000 to 2002 he was a Research Associate at the University of Bristol, U.K., working on hybrid electromagnetic methods for EMC problems in optical transceivers and FDTD analysis of photonic crystals. He was appointed as a lecturer in the department of Electrical and Electronic Engineering at the University of Bristol in 2002 and was made Senior Lecturer in 2007. He has published 39 journal and more than 120 conference papers (11 Invited), in the areas of fabrication, modelling and measurement of photonic crystal based devices, radio-over-fibre, active integrated antennas, FDTD analysis and MMIC design.